ELSEVIER

Journal of Nuclear Materials 264 (1999) 161–168

journal of nuclear materials

Contact corrosion measurements on the pair UO_{2+x} and carbon steel 1.0330 in brines and bentonite porewater with respect to direct waste disposal

J. Engelhardt *, G. Marx

Freie Universität Berlin, Institut für Anorganische und Analytische Chemie, FG Radiochemie, Fabeckstr. 34-36, 14195 Berlin, Germany

Received 31 March 1998; accepted 18 June 1998

Abstract

Contact corrosion between carbon steel and UO_2 was studied in the $MgCl_2$ rich Q-brine, in bentonite porewater and in saturated NaCl solution by use of contact potential and contact current measurements. In all solutions the carbon steel dominates the contact potential, so that this potential is near to the rest potential of the carbon steel. Only in solutions without precipitation of iron corrosion products, the presence of metallic iron slightly reduces the UO_2 corrosion rate. If iron corrosion products precipitate, the relevant adsorption of the uranium species will be more effective than any direct cathodic corrosion protection.

1. Introduction

Germany considers the direct disposal of spent fuel elements in a rock salt formation or in a granite formation to be an alternative to spent fuel processing. With respect to the most serious hypothetical accident to be taken into consideration, namely the intrusion of brines into the disposal area and its contact with the waste package, the corrosion of UO_2 has to be investigated under relevant disposal conditions and at various redox potentials [1–3] in order to get physicochemical data for modelling. For the direct disposal of spent fuel elements the Pollux container will be used for preventing the waste form against the attack of brines for 500 years. The main components of the Pollux container consist of carbon steels [4]. After the penetration of the container which might be happen after approximately 500 years the metallic iron will not be totally corroded, so that it can contact the UO_2. On account of this event the electrochemical behaviour of UO_2 will change, which must be taken into consideration within the frame of safety analysis for the repository. Some leaching experiments [6–8] were done on UO_2 corrosion under the influence of iron or iron corrosion products, which demonstrated that the solubility of UO_2 decreases by adsorption. In most cases the corrosion of UO_2 had not changed because a direct contact was not considered.

In this work, we aimed at more insight into the interaction between carbon steel and UO_2. Our special interest was focused on contact potential measurements of the contact pair carbon steel 1.0330 and UO_2 to compare the behaviour at their relevant rest potentials [3,5].

The value of the contact potential is located between the values of the rest potentials of carbon steel and UO_2, but not directly in the middle of them because it depends on the polarisation resistances of carbon steel and UO_2. The electrode with the lower polarisation resistance dominates the contact potential. Then the contact potential is shifted to the rest potential of the dominating electrode. The behaviour of the dominating electrode itself influences the contact potential, so that this potential can change drastically if the dominating electrode is passivated.

The resulting current which flows between the electrodes being in contact increases the corrosion rate of the anodic part of the contact and can be equal to the difference between the corrosion rates in contact and at

* Corresponding author. Tel.: +49-3 30 838 2461; fax: +49-3 30 838 2463; e-mail: jgengelh@chemie.fu-berlin.de.

0022-3115/99/$ – see front matter
PII: S0022-3115(98)00461-9

rest potential [10]. Presuming a homogeneous potential distribution between the two materials, both the dominant partner and the spot where the cathodic and anodic reactions happen can be determined from contact potential measurements. This is to be correlated to the real attack on the corroded surface obtained from direct-light microscopy.

By measuring the current flowing between the carbon steel and UO_2 during contact it is possible to compare the amount of the current with the corrosion rates of UO_2 and carbon steel. Furthermore, after measuring the rest potential and contact potential, by comparing the change of the corrosion attack on the surface of UO_2 and steel one may get a better insight into the corrosion reaction.

2. Experimental details

2.1. Electrochemical devices

The experimental procedures to carry out rest potential and impedance measurements are described in detail in [1,2,9]. Predicting a homogeneous potential distribution between the contact elements the contact potential can be directly measured [10]. Therefore, a contact has to be made between the carbon steel and UO_2 outside of the solution. Under these conditions both electrodes will have the same potential, which is to be referred to a Ag/AgCl electrode [11,12], if the inner resistance of the solution can be neglected. Being in contact, one of the electrodes will become the anode and the other the cathode, so that a current flows between both electrodes. This current can be measured by use of a potentiostat which adjusts a potential difference between the two electrodes equalling zero. The current needed for this procedure equals the contact corrosion current. It can be recorded by using a high ohmic resistance.

2.2. The specific electrodes used

The types of UO_2 electrodes used were the pellet electrode, which is produced by gluing the UO_2 pellet into a PVC holder, and the 'paraffin electrode', which is made of a mixture of UO_{2+x} powder and paraffin. All electrode types are described in detail in [1–3,9]. The UO_2 electrodes were always abraded before starting the electrochemical experiments. In addition the UO_2 pellet electrodes were polished and cleaned in an ultrasonic bath.

The fine-grained carbon steel 1.0330 (<0.10% C, 0.20–0.45% Mn, <0.035% P, <0.035% S, <0.007% N and very small amounts of Si) [12a] was used as a surrogate for the different types of iron compounds of the Pollux cask. Disks of 1 cm diameter were cut out of plates from this steel and were mounted in a teflon holder. This procedure results in a surface of 0.50 cm^2. The carbon steel electrode was abraded and polished before being mounted.

2.3. The solution parameters

The measurements were made in the $MgCl_2$ rich Q-brine, in bentonite porewater and in saturated NaCl solution (Table 1) at different pH values and under aerobic conditions. The investigations were carried out at 25°C.

2.4. Corrosion measurements

The uranium concentration was determined by using LSC-counting with a Beckmann LSC(LS 6500) and the rotiscint eco plus cocktail (Roth). For these measurements samples were regularly taken out of the cell and measured discontinuously. This method has a detection limit of 1ppm uranium. Uranium concentrations below this limit were detected photometrically with arsenazo III [15,16]. For this procedure samples were also taken out, buffered with standards to pH 2 and measured with a Perkin–Elmer 330 spectrophotometer at 652 nm [17]. This method has a detection limit of 25 ppb. The steel corrosion rates were detected by mass loss measurements. The surface of the used electrodes (carbon steel and UO_2) were examined by using a direct-light microscopy, so that pitting corrosion, trough-shaped corrosion and uniform corrosion could be distinguished.

Table 1
Composition of the solutions used at 25°C

Components	$c_{\text{saturated Nacl}}$ (mol/l)	$c_{\text{Q-brine}}$ (mol/l) [13]	$c_{\text{bentonite porewater}}$ (mmol/l) [14]
NaCl	5.4	0.49	2.96
Na_2SO_4	–	–	9.06
KCl	–	0.64	0.28
$MgCl_2$	–	3.77	0.07
$CaCl_2$	–	–	0.16
$NaNO_3$	–	–	0.11
$MgSO_4$	–	0.29	–

The pH value of the bentonite porewater (pH 3–pH 9) was adjusted by adding 0.1M NaOH or 0.1M HCl.

3. Results

3.1. Behaviour of the specific materials at their rest potentials

The rest potentials of the UO_2 and the carbon steel 1.0330 are listed in Table 2 for the different solutions used. In all solutions a large difference (>600 mV) of the rest potentials can be stated between UO_2 and carbon steel.

Under aerobic conditions the rest potentials of UO_2 are dominated by the built-up of higher oxidised surface layers as for instance shoepite which sometimes can act as a protecting barrier [18,19]. A slight thin surface layer of U_3O_7 is always present. When measuring the rest potential of the carbon steel, iron hydroxide precipitates but not at lower pH values than the saturated NaCl solution at pH 1 to pH 1.5 and in Q-brine at pH 4.5. The behaviour of the rest potentials of the carbon steel 1.0330 can be explained by producing local elements [11] in saturated NaCl solution with pH values about pH 4.5 and in bentonite porewater. Then the carbon steel surface shows the active corroding areas covered with corrosion products, under which an attack on the surface happens in a trough-shaped manner. The other areas of the same carbon steel surface are protecting layers, but they cannot be compared to the well known passive layers as for instance those of titanium alloys or stainless steels. They had no indications of corrosion and only consist of a very thin coloured cover. When the iron hydroxide precipitates the pH value will always shift to more neutral values due to buffering.

3.2. Behaviour at contact potential

In Fig. 1 the contact potentials in saturated NaCl solution at different pH values show that this potential is dominated by the carbon steel. The contact potentials are always near to the rest potential of the carbon steel. There is no difference of this potential behaviour between the UO_2 pellet electrode and the UO_{2+x}/paraffin electrode.

After cutting the contact of UO_2 to carbon steel (see Fig. 2), the rest potential of UO_2 increases again and after a long time it reaches normal values of the UO_2 rest potentials in a similar solution. In case of contact, the corrosion rates of the carbon steel increase drastically (mostly by a factor of 3), but for UO_2 the change of corrosion rates are not significant. In Fig. 3 as an example the time dependence of the mass loss of UO_2 at rest potential is compared with that one being in contact with the carbon steel in saturated NaCl solution at pH 1.5. Due to this contact the UO_2 corrosion rate decreases.

In saturated NaCl solutions with higher pH values and in bentonite porewater, the UO_2 corrosion also increases but there is high adsorption of uranium(VI) on the precipitated iron hydroxide. The remaining uranium concentration in solution is then below 25 ppb, so that the detectable corrosion rate of UO_2 is obtained after dissolving the iron hydroxide precipitate (Table 3).

Especially in the bentonite porewater the precipitated black–brown iron hydroxide covers the UO_2 surface completely, but a direct corrosion of the surface cannot be seen. This can be only explained by assuming an iron oxidation state of mostly +II, because Fe(III) attacks UO_2 drastically [9]. In contradiction to the behaviour at rest potential, the corrosion of the carbon steel surface is always more uniform. A separation into active and passive areas cannot be seen at all. The surface of carbon steel electrodes from experiments in saturated NaCl solution at pH 1.5 and the Q-brine at pH 4.5 has not changed compared to the behaviour at rest potential.

Table 2
Rest potentials of UO_2 and the carbon steel 1.0330 at 25°C

Solution	pH Value	Rest potential of UO_2 (mV)	Corrosion rate of UO_2 ($g\ m^{-2}\ d^{-1}$)	Rest potential of the carbon steel 1.0330 (mV)	Corrosion rate of the carbon steel ($\mu m\ a^{-1}$)
Sat. NaCl	1	605 ± 25 [a]	0.045 ± 0.010 [e]	−314 ± 25 [b]	2350 ± 50
Sat. NaCl	1.5	590 ± 25 [c]	0.41 ± 0.05 [d]	−360 ± 25 [b]	277 ± 10
Sat. NaCl	4.5	565 ± 25 [c]	0.28 ± 0.05 [d]	−385 ± 25 [b]	116 ± 10
Sat. NaCl	5	526 ± 25 [a]	0.018 ± 0.010 [e]	−419 ± 25 [b]	100 ± 20
Sat. NaCl	6	570 ± 25 [c]	0.08 ± 0.03 [d]	−440 ± 25 [b]	70 ± 10
Sat. NaCl	13	544 ± 25 [c]	0.05 ± 0.05 [d]	−300 ± 25 [b]	9 ± 10
Q-brine	4.5	410 ± 25 [a]	0.006 ± 0.005 [e]	−376 ± 25 [a]	31 ± 5
Bentonite porewater	3	408 ± 25 [a]	0.04 ± 0.01 [e]	−356 ± 25 [a]	148 ± 10
Bentonite porewater	9	345 ± 25 [a]	0.013 ± 0.010 [e]	−447 ± 25 [a]	67 ± 10

[a] This work.
[b] [11].
[c] [9].
[d] measured with the UO_{2+x}/paraffin electrode.
[e] measured with the UO_2 pellet electrode.

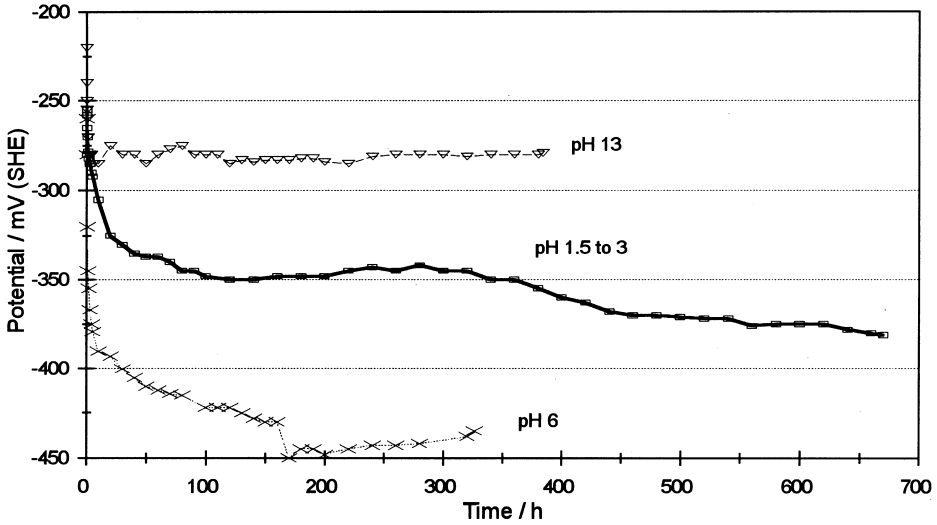

Fig. 1. Time dependence of contact potentials in saturated NaCl solution at 25°C and under the influence of air.

3.3. Impedance measurements

In Fig. 4(a) and (b) impedance spectra of UO_2, carbon steel and their contact are shown. It can be seen that while being in contact the carbon steel dominates the contact behaviour, because the impedance spectra of the contact equal the impedance spectra of the steel itself.

There is no difference at all which kind of UO_2 electrode was used for contacting the steel. The different impedance behaviour of the steel in the saturated NaCl solution at pH 13 and in the bentonite porewater at pH 3 is caused by different states of the steel itself. In the saturated NaCl solution at pH 13 the steel is covered with a thin oxide layer and has a very slow corrosion rate. In bentonite porewater a strong oxygen corrosion of the steel can be seen.

3.4. Contact corrosion current measurements

Contact corrosion current measurements were possible only with the UO_2 pellet electrode, because the inner resistance of the UO_{2+x}/paraffin electrode is too high for current measurements [3].

In Fig. 5 the starting phases (10 h) of the measured contact currents are compared with each other for the different saturated solutions used. Finally after 48 h a

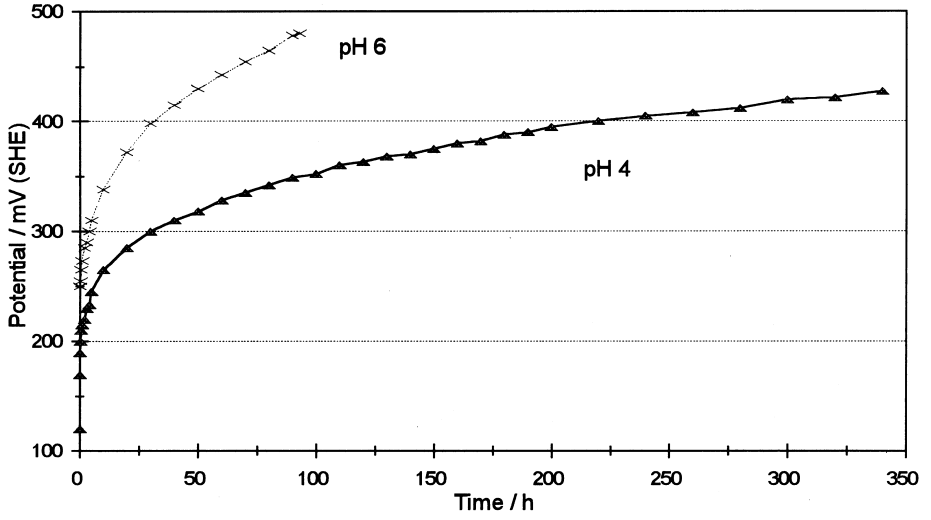

Fig. 2. Time dependence of the UO_{2+x} rest potentials after cutting the contact to the carbon steel.

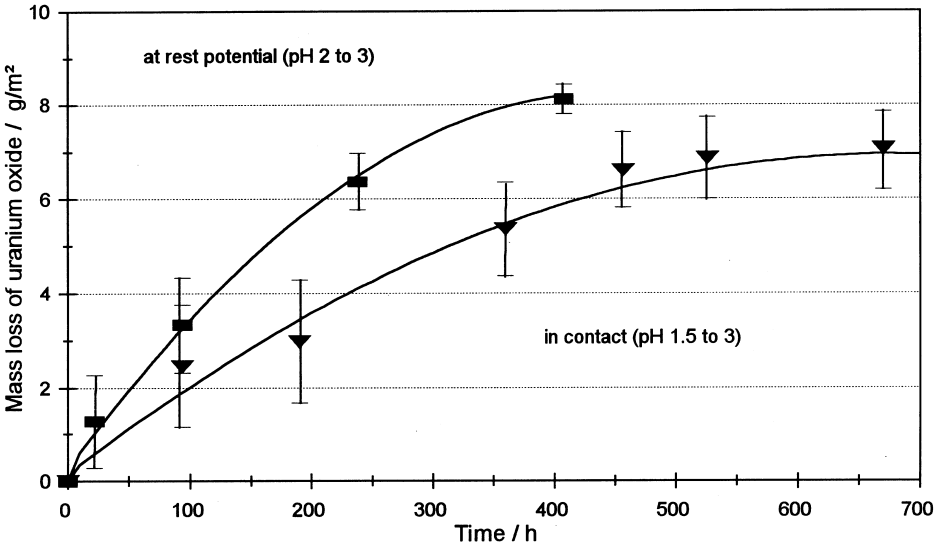

Fig. 3. Time dependence of the UO_{2+x} mass loss in saturated NaCl solution at 25°C and under the influence of air.

constant value is reached. In all cases a cathodic current is obtained, but the value of the current depends on the solution system used. The amount of the current varies up to 25%, so that the current shown in Fig. 5 is an average value. The highest contact corrosion current was obtained in the bentonite porewater (see Table 4) and the lowest in the saturated NaCl solution at pH 1.5, and in Q-brine at pH 4.5. For instance, a current amount of 11.5 μA in bentonite porewater at pH 9 results in a carbon steel corrosion rate of 278 μm/a which is due to a transition of Fe to Fe(II). This current amount equals the increase of the corrosion rate of the carbon steel. The same current amount results in a UO_2 corrosion rate of 19.3 g/m^2 d taking a two-electron step (UO_2–UO_2^{2+}) into consideration. This calculated UO_2 corrosion rate is much higher than the decrease of the corrosion rate, which was experimentally found when UO_2 is in contact with carbon steel and therefore contradicts these experimental results. This point will be explained later on.

These effects are independent of the solution system used, which can be seen in Fig. 6 for the different systems e. g. Q-brine and bentonite porewater at pH 9. In Fig. 6 the measured contact corrosion currents are compared with the calculated currents by using Faraday's law with the analytical iron mass loss of the carbon steel electrodes. The difference between the results at contact potential measurement and the results at the contact current measurements are within the precision of the used methods.

Table 3
Contact potentials and corrosion rates of the pair UO_2-carbon steel 1.0330 at 25°C

Solution	pH Value	Contact potential of the pair UO_2-carbon steel 1.0330 (mV)	Corrosion rate of UO_2 (g m^{-2} d^{-1})	Corrosion rate of the carbon steel (μm a^{-1})
Sat. NaCl	1.5	−400 ± 25	0.26 ± 0.05 [a]	735 ± 15
Sat. NaCl	1.5	−381 ± 25	0.25 ± 0.05 [a]	877 ± 15
Sat. NaCl	6	−435 ± 25	0.06 ± 0.05 [a]	384 ± 15
Sat. NaCl	6	−452 ± 25	<0.03 [a]	170 ± 15
Sat. NaCl	6	−435 ± 25	<0.03 [b]	150 ± 50
Sat. NaCl	13	−290 ± 25	<0.03 [a]	Increase of mass
Sat. NaCl	13	−280 ± 25	<0.05 [a]	8 ± 10
Q-brine	4.5	−392 ± 25	<0.005 [b]	50 ± 10
Bentonite porewater	3	−356 ± 25	0.08 ± 0.02 [b]	683 ± 15
Bentonite porewater	7	−480 ± 25	0.07 ± 0.02 [b]	410 ± 15
Bentonite porewater	9	−406 ± 25	0.024 ± 0.010 [b]	693 ± 15

[a] measured with the UO_{2+x}/paraffin electrode.
[b] measured with the UO_2 pellet electrode.

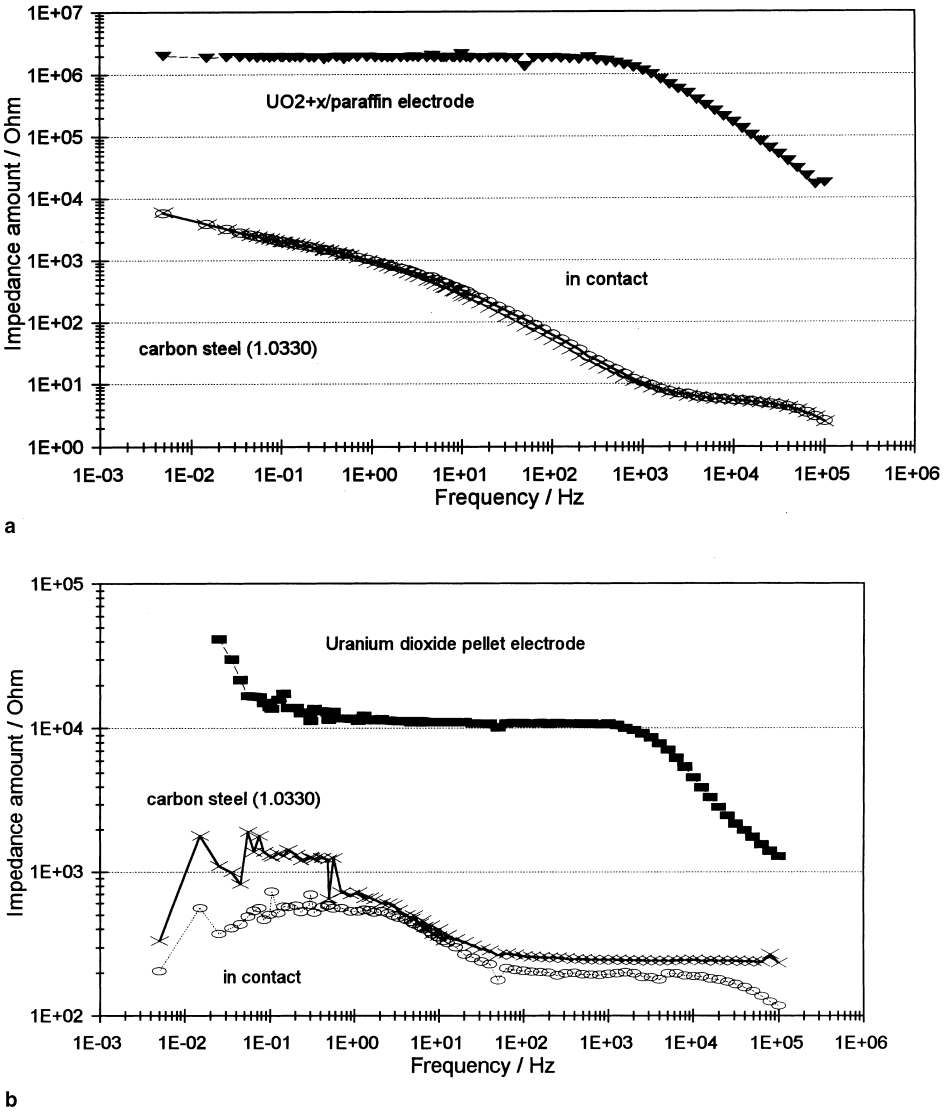

Fig. 4. Impedance spectra at 25°C and under the influence of air; the measured values of the contact potentials were applied. (a) UO_{2+x}/paraffin electrode (▼), carbon steel (×) and their contact (o) in saturated NaCl solution at pH 13 after 400 h; $U_{applied} = -290$ mV (SHE). (b) UO_2 pellet electrode (■), carbon steel (×) and their contact (o) in bentonite porewater at pH 3 after 24 h; $U_{applied} = -400$ mV (SHE).

4. Discussion

The contact of the carbon steel 1.0330 with unirradiated UO_2 influences the electrochemical corrosion behaviour of UO_2. Due to the lack of a passive state of the carbon steel, the dominating behaviour of the carbon steel in contact with UO_2 can be explained by the total different current density-potential behaviour of carbon steel and UO_2 which totally differs from each other.

Over a larger potential range (−500–+200 mV), the semiconducting UO_2 has a small potential-independent current density in the electrolyte solutions used. Only at higher anodic potentials (>+500 mV) the current density and the resulting corrosion rate increase. The exchange current density is very low ($<10^{-10}$ A/cm^2) and the polarisation resistance is high (>0.1 MΩ).

In contradiction to the behaviour of UO_2, the current density-potential behaviour of the carbon steel definitely changes, due to a low polarisation resistance (0.1–20 kΩ) and a higher exchange current density. The polarisation resistance of the carbon steel depends on the cathodic counter reaction, which can be changed by different pH values of the electrolyte solution. In acidified solutions

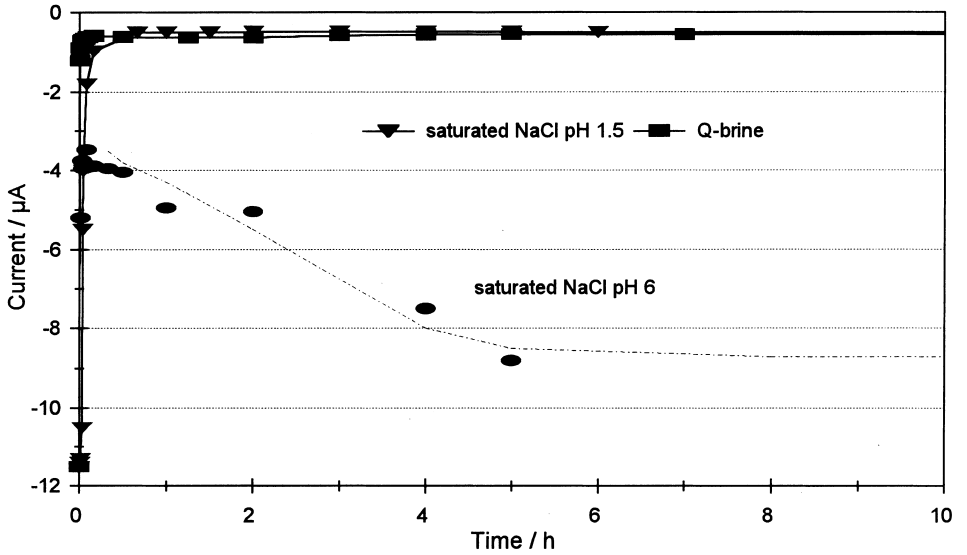

Fig. 5. The first 10 h of the time dependence of contact corrosion current measurements on the pair UO_2-carbon steel at 25°C and under the influence of air.

(pH < 3) the carbon steel corrodes under hydrogen evaluation which happens at each part of the surface and is not inhibited. With increasing pH value this mechanism changes to an oxygen reduction mechanism.

The oxygen reduction produces hydroxide ions, which separate the carbon steel surface to higher and lower corroding spots. These local elements are stabilised by chloride ions and produce a trough-shaped corrosion. This cathodic reaction appears in all solutions used except in the saturated NaCl solution at pH 1.5. These local elements vanish from the carbon steel surface in contact with UO_2 because the cathodic oxygen reduction now happens at the UO_2 surface, an effect which can be seen in unstirred solutions when the precipitation of iron hydroxides appears between the two electrodes as a stria. The UO_2 itself acts as an inert electrode in this case, so that the self corrosion does not change significantly. So the contradiction between the experimental and calculated results of contact current corrosion measurements could be explained.

The resulting cathodic current depends on the oxygen content of the solution which is much higher in the bentonite porewater than in the saturated salt solutions. This results in a higher corrosion rate of the carbon steel in bentonite porewater.

Due to the corroding carbon steel the oxygen content of the solution is reduced. Moreover the solution is buffered by precipitation of iron hydroxides. The influence of the carbon steel being in contact with UO_2 dominates until all iron has been oxidised. The remaining detectable UO_2 corrosion is a complexation and dissolution reaction of higher oxidised uranium, which is

Table 4
The contact current at 25°C in aerobic solutions

Solution	pH Value	Contact current of the pair UO_2-carbon steel 1.0330 (µA)	Corrosion rate of UO_2 (g m^{-2} d^{-1})	Corrosion rate of the carbon steel (µm a^{-1})
Sat. NaCl	1	−0.85 ± 0.05	0.015 ± 0.010	3000 ± 100
Sat. Nacl	1.5	−0.58 ± 0.05	–	–
Sat. NaCl	6	−8.8 ± 0.3	–	–
Sat. NaCl	13	−0.55 ± 0.05	0.023 ± 0.010	13 ± 10
Q-brine	4.5	−0.54 ± 0.05	<0.005	37 ± 15
Q-brine	4.5	−0.52 ± 0.05	–	–
Bentonite porewater	7	−10.9 ± 0.1	0.062 ± 0.010	330 ± 15
Bentonite porewater	9	−6.85 ± 0.1	–	–
Bentonite porewater	9	−9.50 ± 0.05	–	1100 ± 100 [a]
Bentonite porewater	9	−11.4 ± 0.2	–	–

[a] after 30 h measured.

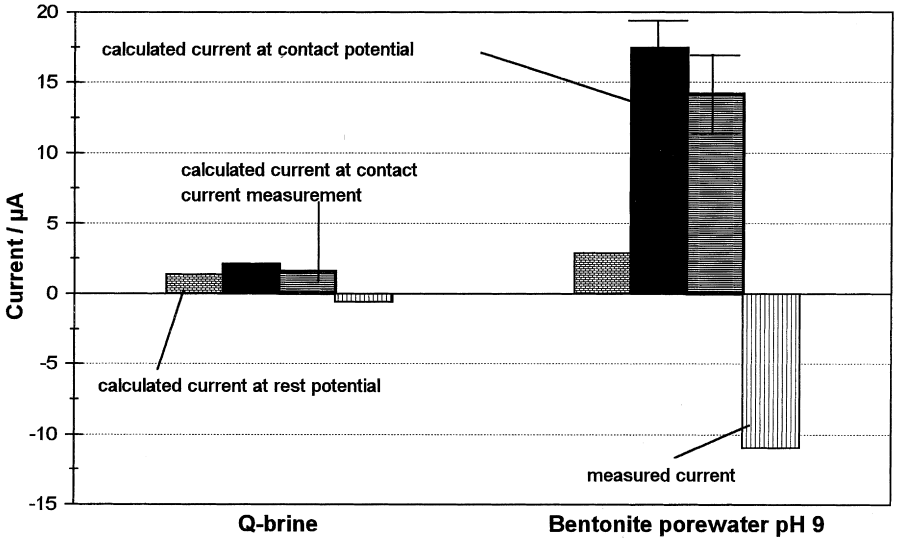

Fig. 6. Comparison between the measured contact current and the calculated current using Faraday's law with the measured corrosion rate for the carbon steel.

always present on the UO_2 surface. This also explains the corrosion rates of the UO_{2+x} lipstick electrode which are higher than those of the UO_2 pellet electrode.

Acknowledgements

This work was partly financially supported by the 'Bundesministerium für Bildung Wissenschaft, Forschung und Technologie (BMBF)', which has been gratefully appreciated.

References

[1] P.-M. Heppner, G. Marx, Radiochim. Acta 58&59 (1992) 21.
[2] G. Marx, J. Engelhardt, F. Feldmaier, M. Laske, Radiochim. Acta 74 (1996) 181.
[3] J. Engelhardt, F. Feldmaier, M. Laske, G. Marx, J. Nucl. Mater. 238 (1996) 104.
[4] Vortragssammlung: Direkte Endlagerung, Report FZKA-PTE 2 der Abschlußveranstaltung 7.12.95–8.12.95 in Karlsruhe.
[5] G. Marx, C. Altenhein-Haese, H. Bishoff, J. Engelhardt, F. Feldmaier, J. Radioanal. Nucl. Chem. 194 (1) (1995) 95.
[6] W.J. Gray, G.L. Vay, J.O. Barner, J.W. Shade, R.W. Cote: in Scientific Basis for Waste Management VII Mater. Res. Soc. Symp. Proc. 76 (1984).
[7] B. Grambow, A. Loida, P. Dressler, H. Geckeis, J. Gago, I. Casas, J. de Pablo, J. Gimenez, M.E. Torrero, FZKA 5702, März, 1996.
[8] B. Grambow, E. Smailos, H. Geckeis, R. Müller, H. Hentschel, Radiochim. Acta 74 (1996) 149.
[9] G. Marx, J. Engelhardt, F. Feldmaier, P.-M. Heppner, Elektrochemische Untersuchungen an unbestrahltem Urandioxid und simuliertem Spent Fuel in endlagerrelevanten Laugensystemen, BMBF-Final Report FKZ 02 E 82711, 1996.
[10] DIN 50919: Korrosionsuntersuchungen der Kontaktkorrosion in Elektrolytlösungen, Dt. Institut f. Normung e.V., Beuth Verlag, 1984.
[11] G. Marx, D. Wegen, J. Engelhardt, BMFT-Abschlußbericht Korrosionsuntersuchungen an Werkstoffen für LAW-Abfallgebinde, FKZ 02 W 61100, Berlin, 1994.
[12] G. Marx, F. Feldmaier, J. Engelhardt, A. Kupfer, Elektrochemische und radiochemische Korrosionsuntersuchungen an UO_2 in endlagerrelevanten Elektrolytsystemen, BMBF-Final Report, FKZ 02E 8725 3, 1998; (a) W. Hauser, B. Fiehn, S. Dronik, D. Wiume, Kernforschungszentrum Karlsruhe Final Report KfK 4300, 1988.
[13] O. Braitsch, Salt deposits, their origin and composition, Springer, Berlin, 1971.
[14] B. Torstenfelt, Radiochim. Acta 39 (1986) 105.
[15] J. Fries, H. Getrost, Organische Reagenzien für die Spurenanalytik, Merck, 1977, p. 352f.
[16] H. Onishi, K. Sekine, Talanta 19 (1972) 473.
[17] W.H. Kim, K.C. Choi, K.K. Park, T.Y. Eom, Radiochim. Acta 66&67 (1994) 45.
[18] R. Wang, B. Katayama, Nucl. Waste Managem. 3 (1982) 83.
[19] D.W. Shoesmith, S. Sunder, M.G. Bailey, G.J. Wallace, Corros. Sci. 29 (1989) 1115.